



3-Methyl-4-substituted Benzylidene Pyrazol-5-ones: Synthesis, Evaluation of Antinociceptive Activities and *in silico* Studies

B. SWAPNA*, SHAHEEN BEGUM, ARIFA BEGUM, K. BHARATHI and D. SUJATHA

Institute of Pharmaceutical Technology, Sri Padmavati Mahila Visvavidyalayam (Women's University), Tirupati-517 502, India

*Corresponding author: E-mail: shaheen.pharmchem@gmail.com

Received: 21 May 2018;

Accepted: 19 June 2018;

Published online: 31 July 2018;

AJC-19029

A series of 3-methyl-4-substituted benzylidene pyrazol-5-ones were subjected to molecular docking studies using targets involved in nociception such as COX-2, TRPV1, P2X3 and glutamate to explore the structural features necessary for interactions with the active site of amino acids in various biological targets. Molecular docking studies showed that the introduction of electron releasing groups on benzylidene ring seem to enhance the binding affinity of pyrazolones. Compounds **M2** (4-hydroxy) and **M8** (3,4-dimethoxy) showed good binding affinity for TRPV1 and P2X3 receptors, whereas compound **M9** (3,4,5-trimethoxy) was found to be favorable for COX-2 and glutamate receptors. These compounds were synthesized and evaluated using capsaicin, ATP and glutamate induced nociception to study the effect of title compounds on TRPV1, purinergic and glutamate receptors, respectively at a dose of 150 mg/kg body weight. Compounds **M6** (3,4-dichloro) and **M8** (3,4-dimethoxy) displayed good antinociceptive activity in TRPV1 and ATP induced nociception models whereas, compound **M9** (3,4,5-trimethoxy) exhibited promising activity in glutamate-induced nociception. Some of the synthesized compounds bearing unsubstituted 4-hydroxy-2,3-dimethoxy and 4-dimethylamino benzylidene ring (**M1-M4**) have been earlier reported for their antinociceptive activity in acetic acid induced writhing and tail immersion methods. The results of the present study implicated that the compounds possessing 4-hydroxy and 4-dimethylamino groups showed good antinociceptive activity in all the models. The results might be useful to design and develop pyrazolones as potential antinociceptive agents.

Keywords: Pyrazolones, COX-2, P2X3, Capsaicin model, ATP-induced nociception, Glutamate induced model.

INTRODUCTION

Pain management remains challenging irrespective of the various recent advancements in the development of potential antinociceptive agents. Research in this area revealed involvement of diverse targets such as receptors, neurotransmitters, voltage-gated sodium and potassium ion channels and enzymes, indicating complex nature of pain mechanisms. Some important receptors include cannabinoid (CB1 and CB2) imidazoline-2 (I_2), adenosine, purinergic (P2X3 and P2X7), transient receptor potential vanilloid (TRPV) and ankyrin (TRPA) and neurotransmitters such as bradykinin, prostaglandin E_2 , tumor necrosis factor alpha (TNF- α), interleukin (IL)-1 and nitric oxide. Soluble epoxide hydrolase (eSH), cyclooxygenase-2 (COX-2) nitric oxide synthase (NOS) and enzymes related to endocannabinoid system like fatty acid amide hydrolase (FAAH), monoacylglycerol lipase (MAGL) are potential targets for antinociceptive drug development [1-9].

Narcotic analgesics, nonsteroidal anti-inflammatory drugs (NSAIDs) and several other non-specific analgesics such as antidepressants, local anesthetics and anticonvulsants are used to treat a range of pain conditions. Recently, approved drugs such as ziconotide (N-type calcium channel inhibitor), ketamine (NMDA antagonist) and dronabinol (CB1 & CB2 agonist) exhibit antinociceptive activity by acting through novel mechanisms, indicating the importance of newer targets for pain. Limited clinical effectiveness of the available antinociceptive drugs is the major driving force to search newer and effective antinociceptive drugs [10].

Pyrazolone represents an important scaffold to design and develop molecules with antinociceptive and antipyretic activities. Antipyrine, an analgesic drug and several NSAIDs such as phenylbutazone, oxyphenbutazone and aminophenazone possess pyrazolone moiety in their structure [11]. Compounds possessing pyrazolone ring have been extensively described for their diverse pharmacological activities *viz.*, antipyretic, antinocicep-

tive, anti-inflammatory, antiviral and antioxidant activities [12-15]. Pyrazolone containing drugs such as dipyron exhibit antinociceptive activity by inhibiting transient receptor potential ankyrin (TRPA1) and adenosine 5' tri phosphate (ATP)-induced calcium responses indicating that pyrazolones can modulate the activity of TRP and ATP receptors [16,17].

Several antimicrobial, antinflammatory, antinociceptive and cytotoxic compounds possess arylidene or heteroarylidene ring in their structure, indicating the pivotal role of arylidene ring for the activity. In general, introduction of substituted benzylidene/arylidene ring enhances the biological activities of parent structure which might be due to the lipophilicity and favourable steric effects imparted by arylidene scaffold [18-20].

3-Methyl-4-substituted benzylidene pyrazol-5-ones were reported to exhibit antinociceptive activity in acetic acid induced writhing and tail-flick methods [14,15]. It was found interesting to probe the detailed antinociceptive mechanisms of these compounds. Molecular docking is an efficient *in silico* tool which provides an insight into ligand-target interactions and reveal electrostatic as well as steric complementarity between the target structure and ligand molecule. Prompted by the usefulness of molecular docking studies, 3-methyl-4 substituted benzylidene pyrazol-5-ones (M1-M9) were docked into the active sites of targets (COX-2, TRPV1, glutamate and P2X3) related to antinociceptive activity. Based upon the molecular docking results, a series of 3-methyl-4-substituted benzylidene pyrazol-5-ones were synthesized and screened for antinociceptive activity using nociception models such as capsaicin, glutamate and ATP-induced nociception models. In addition, molecular properties and pharmacokinetic properties were calculated to predict oral bioavailability, absorption, distribution and CNS permeation which might be correlated to biological activities displayed by the title compounds.

EXPERIMENTAL

Hydrazine hydrate, ethylacetoacetate and different aldehydes were purchased from Sigma-Aldrich chemicals. All other chemicals are of AR grade. The melting points were determined in one-end-open capillary tubes on a "Thermonik Precision Melting point cum Boiling point apparatus, Model C-PMB-2 and were uncorrected. The purities of the compounds were monitored by TLC using precoated aluminium sheets (Merck), coated with silica gel (Keisel gel 60). The spots were developed in an iodine chamber and visualized under ultra-violet (UV) spectra chamber. The IR spectra were obtained using KBr pellets on Perkin-Elmer Spectrum-BX-I infrared spectrophotometer (cm^{-1}). The ^1H NMR spectra were recorded in CDCl_3 on Bruker-400 MHz or Jeol-400MHz instrument. Mass (m/z) spectra were obtained using LCMS-8030 mass spectrometer with mass selective detector.

Molecular docking studies: SwissDock (<http://swissdock.vital-it.ch/>), was used for performing molecular docking studies [21]. Ligand molecules (M1-M9) were built using Chem Draw 12 version and saved in mol2 format whereas crystal structures of proteins (COX-2: PDBID: 3LN1; P2X3 PDBID: 5SVJ; TRPV1: PDBID: 2PNN; glutamate: PDBID: 3RN8) were retrieved from Protein Data Bank. Protein structure for P2X3 *i.e.* 5SVJ was prepared using "dock prep" module (solvent molecules are removed; hydrogens and partial charges are added)

available in chimera and others were directly submitted for the docking study. To compare the results, respective inbuilt ligands were selected for the docking studies [COX-2: celecoxib; P2X3: adenosine triphosphate (ATP); TRPV1: adenosine triphosphate (ATP); glutamate: 3,3'-benzene-1,4-diylbis(4-cyano-5-ethylthiophene-2-carboxylic acid (RN8)].

Whole protein structure was selected for the docking. The predicted binding modes with most favourable energies were evaluated with fast analytical continuum treatment of solvation (FACTS) in SwissDock module and clustered. The most favourable clusters can be visualized using the View Dock plug-in of UCSF chimera. Gibbs free energy (ΔG) and fullfitness energies were calculated for each molecule in the protein complex.

Pharmacology: Adult male Wistar rats (200-240 g) were obtained from Sri Venkateswara Enterprises, Bangalore, India. They were kept in a temperature controlled environment ($25 \pm 2^\circ\text{C}$) with a 12 h light-dark cycle with access to food and water *ad libitum*. All animal experimental protocols were approved by Institutional Animal Ethical Committee (IAEC) of Sri Padmavati Mahila University, (1677/PO/Rs/S/2012/CPCSEA/28), Tirupati, India. The following three antinociceptive models were used to evaluate the synthesized compounds (M1-M9). The compounds were suspended well in 1 % sodium carboxymethyl cellulose solution freshly before administration to animals.

Capsaicin induced nociception model: In this test, nociception was induced by administering 20 L of capsaicin (1.6 $\mu\text{g/paw}$) onto the intraplantar region of the right hind paw of rat [22]. The animals were treated with synthesized compounds (150 mg/kg p.o) 60 min prior to capsaicin injection. The rats were placed in a Plexiglas cage (30 20 20 cm). The amount of time spent licking the injected paw was recorded after 5 min following the injection of capsaicin.

Adenosine 5'-triphosphate (ATP) induced paw licking test: In this test, nociception was induced by administering 0.125 mg/mL of ATP [23] and the time spent and number of licking/flinching to the injected paw, was considered as the indicators of pain and registered separately at 0-10 min. The control animals received a similar volume of saline.

Glutamate induced paw licking test: The animals were treated with synthesized compounds (150 mg/kg p.o) one hour before the glutamate injection. Nociception was induced by administering 20 L of 30 mol glutamate into the intraplantar region of the right hind paw of rat [24]. After injection of glutamate, the rats were observed for 15 min post injection and the time spent and number of licking the injected paw was recorded and considered as nocifensive behaviour.

Statistical analysis: The results were presented as mean \pm SD. The statistical significance was analyzed by analysis of variance followed by Dunnett's multiple comparison test. P-values of less than 0.05 were considered as indicative of significance.

Prediction of Molecular and ADME descriptors: Molecular descriptors [$\log P$ (partition coefficient), molecular weight, hydrogen bond acceptors and donors a molecule and topological polar surface area (TPSA)] were calculated using the online software (<http://www.molinspiration.com/>). Pharmacokinetic properties were predicted using preADMET online server (<http://preadmet.bmdrc.org/>), which calculates the human intestinal absorption,

in vitro Caco-2 cell permeability, Maden Darby Canine Kidney (MDCK) cell permeability, skin permeability, plasma protein binding and blood brain barrier penetration (BBB) [25]. The drug absorption percentage [26] was estimated using the following equation:

$$\text{ABS (\%)} = 109 - (0.345 \times \text{TPSA})$$

RESULTS AND DISCUSSION

A series of 3-methyl-4-substituted benzylidene pyrazol-5-ones (**M1-M9**) were synthesized by condensing 3-methyl pyrazol-5-one with various substituted aromatic aldehydes (**Scheme-I**). The title compounds were obtained in good yields. The IR spectra of the compounds displayed characteristic absorption bands in the regions 2850-2840 cm^{-1} (C-H arom.), 1648-1600 cm^{-1} (C=O), 1586-1500 cm^{-1} (C=C). The $^1\text{H NMR}$ spectra of the title compounds showed the signals of aromatic hydrogens and methane protons as multiplets between 6.8-8.3 ppm. The mass spectra of the compounds showed the characteristic M^+ or $[\text{M}+\text{H}]^+$ peaks.

Spectral data

4-Benzylidene-3-methyl-1H-pyrazol-5-(4H)-one (M1): m.f. $\text{C}_{11}\text{H}_{10}\text{N}_2\text{O}$, m.p. 242-244 °C (lit. 240-242 °C); Elemental analysis (Found) %: C, 70.90; H, 5.42; N, 15.03; O, 8.57. FT-IR (KBr, ν_{max} , cm^{-1}): 3486.50 (N-H *str.*), 2826.24 (C-H arom. *str.*), 2654.21 (C-H aliph. *str.*), 1693.79 (C=O *str.*), 1585.87 (C=C *str.*); $^1\text{H NMR}$ (CDCl_3 , δ ppm): 2.21 (s, 3H, CH_3), 6.68-7.28 (m, 4H, Ar-H & benzylidene), 8.05 (s, 1H, NH). MS (m/z): 186 $[\text{M}]^+$; 187 $[\text{M}+\text{H}]^+$.

4-(4-Hydroxybenzylidene)-3-methyl-1H-pyrazol-5-(4H)-one (M2): m.f. $\text{C}_{11}\text{H}_{10}\text{N}_2\text{O}_2$, m.p. 208-210 °C (lit. 212-214 °C); Elemental analysis (Found) %: C, 65.37; H, 4.96; N, 13.82; O, 15.81. FT-IR (KBr, ν_{max} , cm^{-1}): 3469.06 (O-H *str.*),

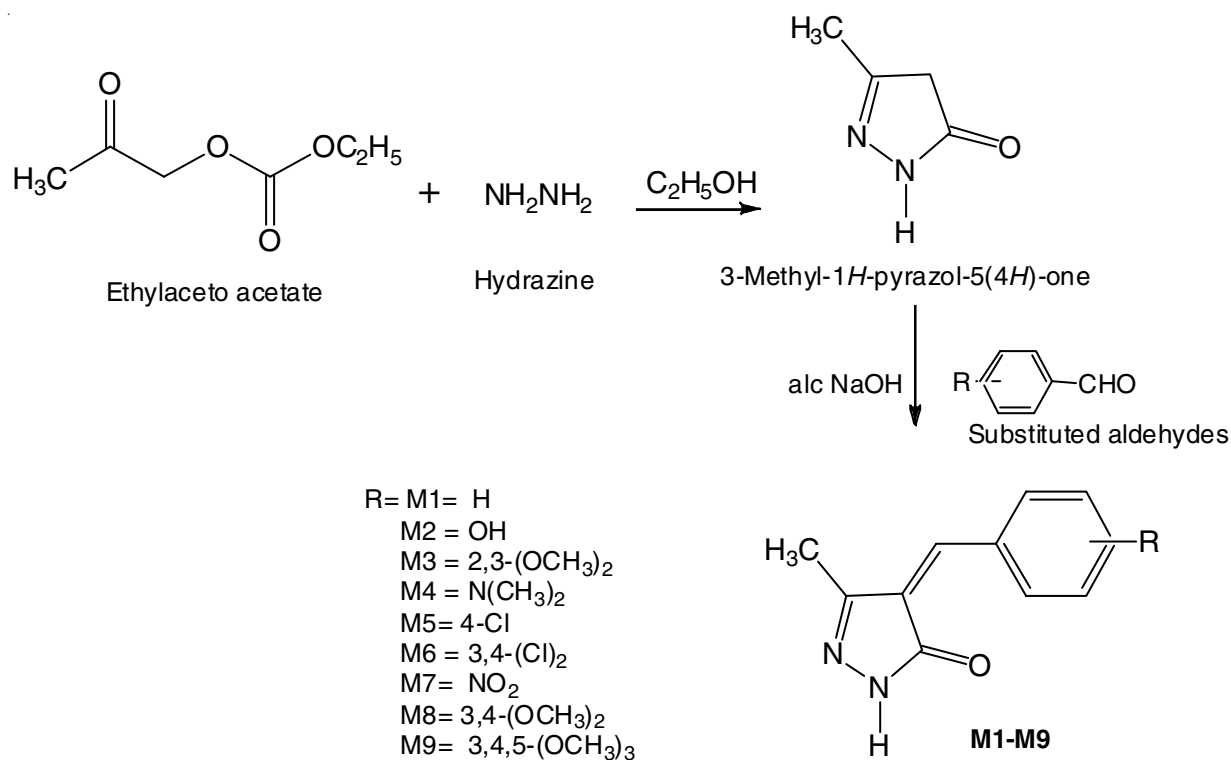
2878.45 (C-H arom. *str.*), 2829.67 (C-H aliph. *str.*), 1670.41 (C=O *str.*), 1596.33 (C=C *str.*); $^1\text{H NMR}$ (CDCl_3 , δ ppm): 1.92 (s, 3H, CH_3), 6.13 (s, 1H, benzylidene), 6.61-7.11 (m, 4H, Ar-H), 8.05 (s, 1H, NH). MS (m/z): 202 $[\text{M}]^+$, 203 $[\text{M}+\text{H}]^+$.

4-(2,3-Dimethoxybenzylidene)-3-methyl-1H-pyrazol-5-(4H)-one (M3): m.f. $\text{C}_{13}\text{H}_{14}\text{N}_2\text{O}_3$, m.p. 205-207 °C (lit. 208-210 °C); Elemental analysis (Found) %: C, 63.38; H, 5.72; N, 11.36; O, 19.47. FT-IR (KBr, ν_{max} , cm^{-1}): 3376.65 (N-H *str.*), 2985.87 (C-H arom. *str.*), 2849.84 (C-H aliph. *str.*), 1678.23 (C=O *str.*), 1569.79 (C=C *str.*); $^1\text{H NMR}$ (CDCl_3 , δ ppm): 1.89 (s, 3H, CH_3), 3.01 (s, 6H, $(\text{OCH}_3)_2$), 6.21 (s, 1H, benzylidene), 6.59-7.25 (m, 3H, Ar-H), 8.09 (s, 1H, NH); MS (m/z): 202 $[\text{M}]^+$, 203 $[\text{M}+\text{H}]^+$.

4-[4-(Dimethylamino)benzylidene]-3-methyl-1H-pyrazol-5-(4H)-one (M4): m.f. $\text{C}_{13}\text{H}_{15}\text{N}_3\text{O}$, m.p. 242-244 °C (lit. 236-238 °C); Elemental analysis (Found) %: C, 68.01; H, 6.58; N, 18.35; O, 6.97; FT-IR (KBr, ν_{max} , cm^{-1}): 3368.89 (N-H *str.*), 2988.43 (C-H arom. *str.*), 2849.87 (C-H aliph. *str.*), 1679.41 (C=O *str.*), 1588.68 (C=C *str.*); $^1\text{H NMR}$ (CDCl_3 , δ ppm): 1.92 (s, 3H, CH_3), 3.81 (s, 6H, $\text{N}(\text{CH}_3)_2$), 6.18 (s, 1H, benzylidene), 6.59-7.67 (m, 3H, Ar-H), 8.10 (s, 1H, NH); MS (m/z): 229 $[\text{M}]^+$, 230 $[\text{M}+\text{H}]^+$.

4-(4-Chlorobenzylidene)-3-methyl-1H-pyrazol-5-(4H)-one (M5): m.f. $\text{C}_{11}\text{H}_9\text{N}_2\text{OCl}$, m.p. 210-212 °C; Elemental analysis (Found) %: C, 59.77; H, 4.10; Cl, 16.05; N, 12.71; O, 7.21. FT-IR (KBr, ν_{max} , cm^{-1}): 3420.98 (N-H *str.*), 2923.46 (C-H arom. *str.*), 2859 (C-H aliph. *str.*), 1690.00 (C=O *str.*), 1587.08 (C=C *str.*); $^1\text{H NMR}$ (CDCl_3 , δ ppm): 1.89 (s, 3H, CH_3), 6.18 (s, 1H, benzylidene), 6.35-7.41 (m, 4H, Ar-H), 8.11 (s, 1H, NH); MS (m/z): 220 $[\text{M}]^+$, 221 $[\text{M}+\text{H}]^+$.

4-(3,4-Dichlorobenzylidene)-3-methyl-1H-pyrazol-5-(4H)-one (M6): m.f. $\text{C}_{11}\text{H}_8\text{N}_2\text{OCl}_2$, m.p. 220-222 °C; Elemental analysis (Found) %: C, 51.60; H, 3.15; Cl, 27.82; N, 10.99; O,



Scheme-I: Synthesis of 3-methyl pyrazol-5-one derivatives

6.29. FT-IR (KBr, ν_{\max} , cm^{-1}): 3427.37(N-H *str.*), 3073.51 (C-H arom. *str.*), 2926.09 (C-H aliph. *str.*), 1609.41 (C=O *str.*), 1519.88 (C=C *str.*), 1012.65 (C-Cl *str.*); $^1\text{H NMR}$ (CDCl_3 , δ ppm): 1.90 (s, 3H, CH_3), 6.18 (s, 1H, benzylidene), 6.50-7.25 (m, 3H, Ar-H), 8.13 (s, 1H, NH); MS (m/z): 255 [$\text{M}]^+$, 257 [$\text{M}+\text{H}]^+$.

4-(4-Nitrobenzylidene)-3-methyl-1H-pyrazol-5(4H)-one (M7): m.f. $\text{C}_{11}\text{H}_9\text{N}_3\text{O}_3$, m.p. 182-184 °C; Elemental analysis (Found) %: C, 57.19; H, 3.90; N, 18.12; O, 20.70. FT-IR (KBr, ν_{\max} , cm^{-1}): 3453.37(N-H *str.*), 2998.02 (C-H arom. *str.*), 2826.09 (C-H aliph. *str.*), 1615.58 (C=O *str.*), 1575.45 (C=C *str.*), 1428.73 (N-O assym. *str.*), 1227.48 (N-O sym. *str.*); $^1\text{H NMR}$ (CDCl_3 , δ ppm): 1.92 (s, 3H, CH_3), 6.18 (s, 1H, benzylidene), 6.59-7.54 (m, 4H, Ar-H), 8.11 (s, 1H, NH); MS (m/z): 232 [$\text{M}+\text{H}]^+$.

4-(3,4-Dimethoxybenzylidene)-3-methyl-1H-pyrazol-5(4H)-one (M8): m.f. $\text{C}_{13}\text{H}_{14}\text{N}_2\text{O}_3$, m.p. 216-218 °C; Elemental analysis (Found) %: C, 63.47; H, 5.71; N, 11.36; O, 19.47. FT-IR (KBr, ν_{\max} , cm^{-1}): 3392.67 (N-H *str.*), 2960.87 (C-H arom. *str.*), 2840.13 (C-H aliph. *str.*), 1656.06 (C=O *str.*), 1622.66 (C=C *str.*); $^1\text{H NMR}$ (CDCl_3 , δ ppm): 1.90 (s, 3H, CH_3), 3.02 (s, 6H, $(\text{OCH}_3)_2$), 6.17 (s, 1H, benzylidene), 6.46-7.48 (m, 3H, Ar-H), 8.09 (s, 1H, NH); MS (m/z): 202 [$\text{M}]^+$, 205 [$\text{M}+\text{H}]^+$.

3-Methyl-4-(3,4,5-trimethoxybenzylidene)-1H-pyrazol-5(4H)-one (M9): m.f. $\text{C}_{14}\text{H}_{16}\text{N}_2\text{O}_4$, m.p. 209-211 °C; Elemental analysis (Found) %: C, 60.87; H, 5.82; N, 10.13; O, 23.17. FT-IR (KBr, ν_{\max} , cm^{-1}): 3405.27(N-H *str.*), 2909.04 (C-H arom. *str.*), 2836.77 (C-H aliph. *str.*), 1667.70 (C=O *str.*), 1597.94 (C=C *str.*); $^1\text{H NMR}$ (CDCl_3 , δ ppm): 1.88 (s, 3H, CH_3), 3.08 (s, 9H, $(\text{OCH}_3)_3$), 6.18 (s, 1H, benzylidene), 6.35-7.62 (m, 2H, Ar-H), 8.08 (s, 1H, NH); MS (m/z): 206 [$\text{M}+\text{H}]^+$.

Molecular docking studies: 3-Methyl-4-substituted benzylidene pyrazol-5-ones were previously reported to possess antinociceptive activity. SAR revealed that presence of 4-hydroxy (**M2**)/2,3-dimethoxy (**M3**)/4-dimethylamino groups (**M4**) on benzylidene ring increase the potency of the parent structure (**M1**) [14]. Molecular docking studies were performed to predict affinities and binding modes of these derivatives towards few nociceptive receptors (COX-2, P2X3, TRPV1 and glutamate). The objective of the study was to identify the effect of substituent groups on binding affinity.

COX-2 Enzyme: COX-2, inducible form of cyclooxygenase (COX) enzyme is a validated target for the development of antiinflammatory and antinociceptive agents. COX-2 enzyme contain large solvent accessible surface in the active site; amino acids such as Val-523, Arg-513, Arg-120, Tyr-355 and Glu-524 are situated around the active site.

Results of the molecular docking studies revealed that 2,3-dimethoxy benzylidene derivative (**M3**) showed most favourable interaction with ΔG of -7.79 kcal/mol whereas unsubstituted derivative (**M1**) showed poor interaction with ΔG of -7.37 kcal/mol indicating that methoxy substitution is favourable for binding at the COX-2 enzyme. 4-Dimethylamino or 4-hydroxy benzylidene derivatives (**M2** and **M4**) showed ΔG of -7.59 kcal/mol. Results were compared using celecoxib which showed highest binding affinity with ΔG of -10.15 kcal/mol. Celecoxib was found to establish hydrogen bonding with amino acid residue Phe-504 and Arg-499. The pyrazolones were found to be located at the loop region (Arg-499-Pro-514) and arylidene ring was found to be embedded by amino acids such as Ala-327, Phe-42,

Val-339 and Val-332. Binding modes of the studied pyrazolones were found to be similar to that of celecoxib and most of them were found to interact with Phe-504 amino acid residue. Pyrazolones possessing phenylurea or phenylthiourea, interact with different amino acid residues (π - π stacking of phenyl ring with Trp-387 and Tyr-385) indicating that pyrazolones affinity for COX-2 enzyme is influenced/effected with substitution [27].

As the title compounds exhibited good binding affinity towards the target enzyme, we have designed few more pyrazolones by introducing different functional groups such as 4-Cl, 3,4-Cl₂, 4-NO₂, 3,4-(OCH₃)₂ and 3,4,5-(OCH₃)₃ on benzylidene ring (**M5-M9**) and performed molecular docking studies, to study the importance of substitution on benzylidene ring.

Among methoxy containing derivatives, 3,4-dimethoxy benzylidene derivative (**M8**) exhibited good binding affinity ($\Delta G = -7.96$ kcal/mol) indicated that position of methoxy groups is critical for binding at the active site of receptor. 4-Chloro and 3,4-dichloro substituted derivative and 4-nitro derivatives (**M5**, **M6** and **M7**) showed moderate interactions ($\Delta G = -7.56$ and -7.57 kcal/mol) when compared to unsubstituted derivative (**M1**) ($\Delta G = -7.37$ kcal/mol), suggesting that presence of halogen increases binding affinity. Binding mode of celecoxib and derivative **M8** with COX-2 is shown in Fig. 1.

P2X3 receptors: The purinergic receptor P2X ligand-gated ion channel 3 (P2X3) is highly expressed by nociceptive sensory neurons and involved in pain processing and inflammation. When ATP binds to P2X3 ion channel, it leads to an increase in Ca^{2+} concentration ultimately membrane depolarization. The development of ligands that selectively activate or block specific P2X receptor subtypes represents a promising strategy to develop new drugs for the treatment of pain, cancer, inflammation and neurological diseases [28,29].

4-Hydroxy benzylidene derivative (**M2**) showed highest binding interaction with -7.18 kcal/mol indicated that hydrogen binding ability is favourable for the binding interaction which is comparable to the standard drug ATP (-8.55 kcal/mol). Unsubstituted derivative (**M1**) showed poor interaction towards this receptor (-6.77 kcal/mol), which was found to increase with the presence of either electron releasing substituent groups or electron withdrawing substituent groups on benzylidene ring indicating that substituent groups on benzylidene ring favours binding. Among the compounds, 3,4-dimethoxy (**M8**), 3,4-trimethoxy derivative (**M9**) showed good binding affinity (-6.97 and -6.99 kcal/mol) indicating the importance of methoxy groups on benzylidene ring. Halogen bearing derivatives, 4-nitro derivative and 4-dimethylamino derivatives exhibited moderate interactions with the target receptor. Pyrazolones were found to be located at the loop region (Leu249-Cys256) and most of the compounds were able to establish hydrogen bonding with NH of Asp-248 with oxygen atom present in the pyrazolone ring. Binding mode of ATP and derivative **M3** with P2X3 receptor is shown in Fig. 2.

TRPV1 ion channel: TRPV1 or vanilloid receptor 1 can be activated by eicosanoids, capsaicin, protons and resiniferatoxin [27]. It is expressed by primary afferent sensory neurons of the pain pathway and plays pivotal role in nociception and neurogenic inflammation [30-32]. Results of the molecular

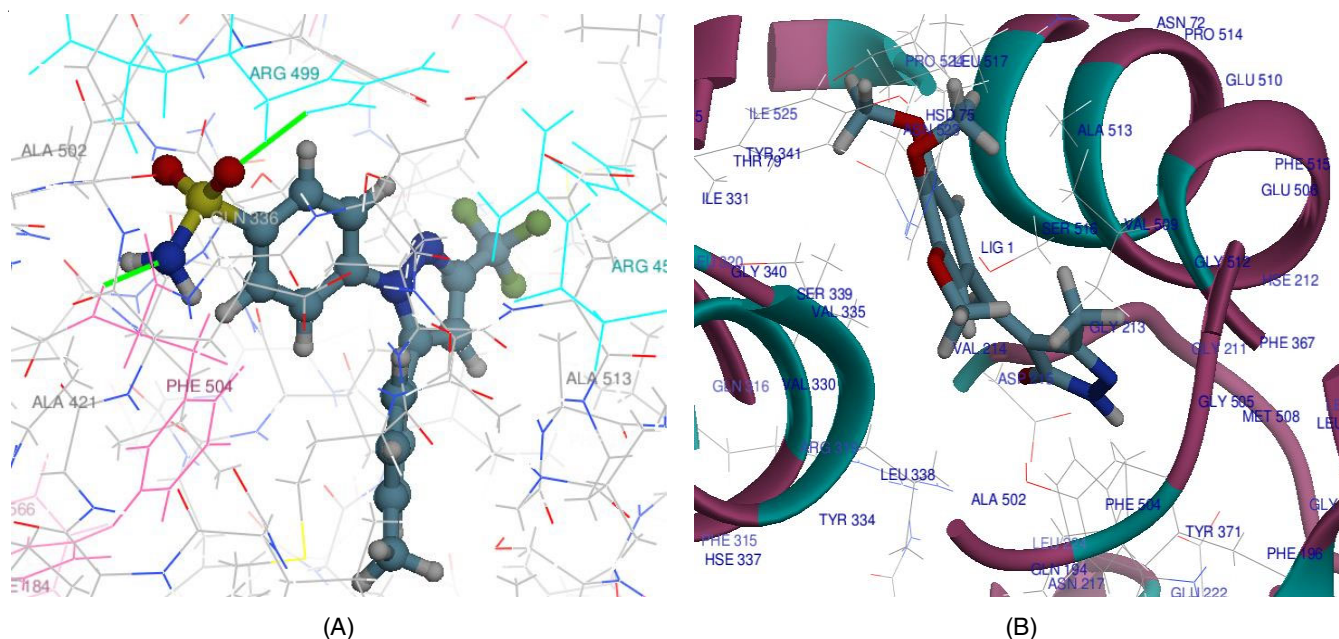


Fig. 1. (A) Predicted binding interactions of celecoxib (B) binding interactions of M8 in COX-2 active site

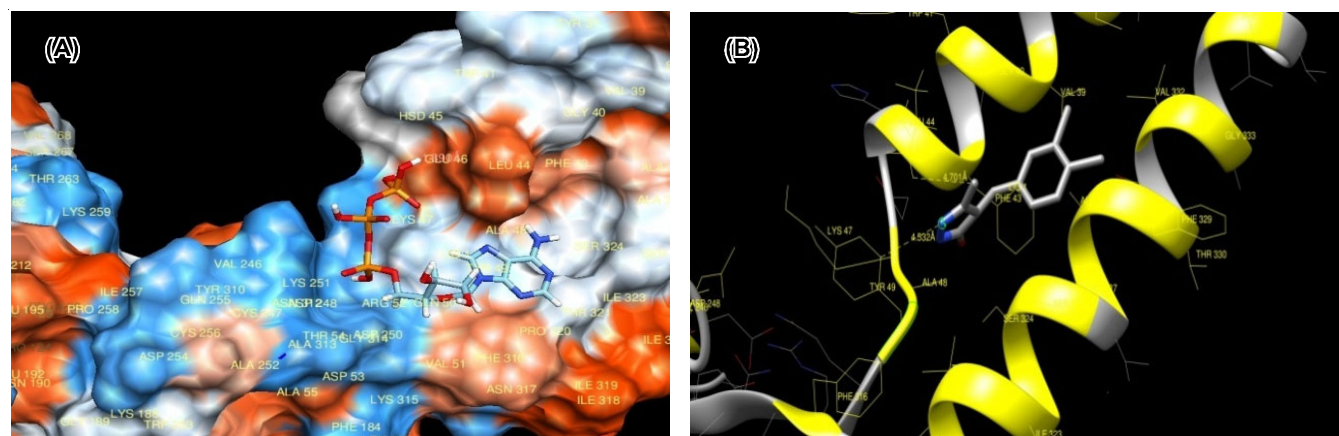


Fig. 2. (A) Predicted binding interactions of ATP (B) binding interactions of M3 in P2X3 receptor

docking study showed that 3,4-dimethoxy benzylidene derivative (**M8**) has good interaction towards TRPV1 receptor (-7.04 kcal/mol) whereas standard inhibitor ATP displayed highest binding interaction (-9.58 kcal/mol). When compared to 2,3-dimethoxy derivative (-6.80 kcal/mol) and 3,4,5-trimethoxy derivative (6.76 kcal/mol), 3,4-dimethoxy derivative showed good interaction and affinity for the receptor which reveals the importance of position of methoxy groups. The results showed that the presence of hydroxy group also increased the binding interactions (-6.95 kcal/mol) when compared to unsubstituted derivative (-6.57 kcal/mol).

In the best binding mode, ATP (Fig. 3) was found to establish hydrogen bonding with Glu-293 and Lys-238 whereas pyrazolones showed similar binding pose as that of ATP in the active site of receptor. Compound **M8** showed the highest binding interaction, was found to interact with Lys-238 *via* hydrogen bonding using pyrazolone carbonyl group.

Glutamate receptors: Metabotropic glutamate receptors (mGluRs) are activated by L-glutamate and recent studies of mGluRs have established glutamate receptors as promising targets in the therapy of psychiatric and pain disorders.

Pyrazolones possessing piperidine or substituted piperidine are patented for the mGluR agonistic activity [33-35]. Among the title compounds, compounds **M8** and **M9** exhibited good interactions with the glutamate receptor with ΔG values -7.99 and -8.01 kcal/mol, respectively. As indicated in Tables 1 and 2, methoxy derivatives were found to be more favourable towards all the studied receptors. Halogenated, nitro derivative, dimethyl-amino derivative showed moderate binding interactions. 3,3'-Benzene-1,4-diylbis(4-cyano-5-ethylthiophene-2-carboxylic acid (RN8), inbuilt ligand, was found to interact with Lys-151 and Lys-144 amino acid residues at the active site and binding poses of pyrazolones indicated that their binding modes are different from the standard ligand. Most of the derivatives were found to establish hydrogen bonding with Asn-242 or Ser-108 (Fig. 4).

Molecular docking results (Tables 1 and 2) showed that 3-methyl-4-substituted benzylidene pyrazol-5-ones showed good binding affinity towards the selected targets. Unsubstituted derivative (**M1**) showed poor binding affinity when compared to various substituted benzylidene derivatives towards all the studied receptors, suggesting that substitution either with

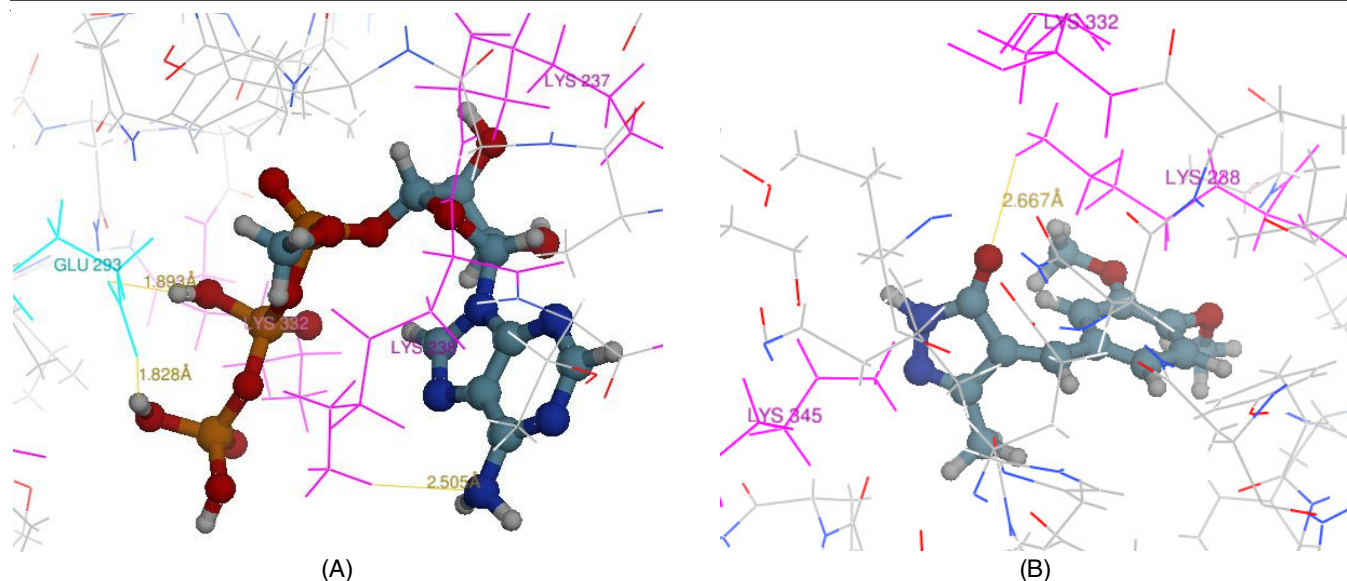


Fig. 3. (A) Predicted binding interactions of ATP (B) binding interactions of M8 in the active site of TRPV1

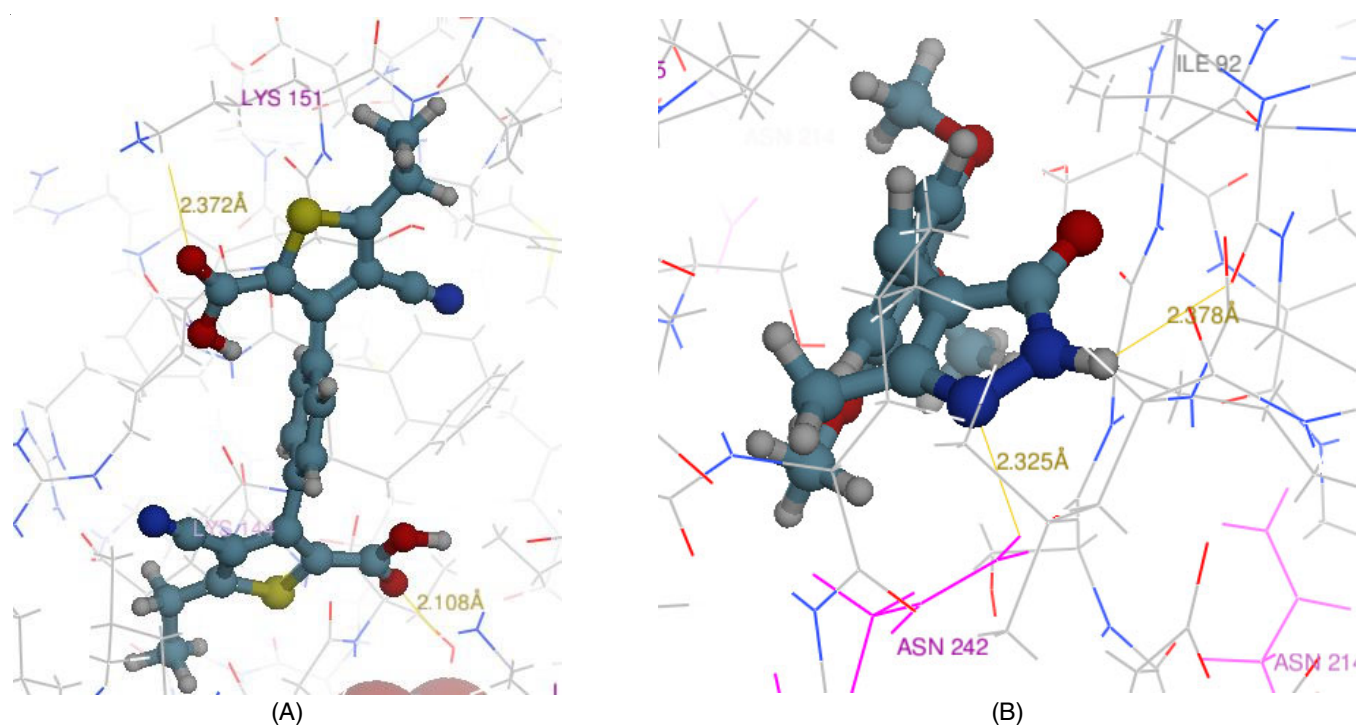


Fig. 4. (A) Predicted binding interactions of RN8 (B) M9 interactions in glutamate receptor

TABLE-1
DOCKING SCORE AND DETAILS OF DOCKING RESULTS OBTAINED USING SWISS DOCK

S. No.	R	COX-2		Interacting residues	P2X3		Interacting residues
		Energy (ΔG)	Full fitness		Energy (ΔG)	Full fitness	
Cel	–	–9.12	–2238.98	Arg-499 Phe-504	–8.55	1989.12	Lys-47 Lys-251 Asp-248
M1	H	–7.37	–2254.55	–	–6.77	–531.10	Asp-248
M2	4-OH	–7.59	–2237.97	Phe-504	–7.18	–541.35	Asp-248
M3	2,3-(OCH ₃) ₂	–7.79	–2224.73	Phe-504	–6.65	–1506.13	Asp-248
M4	4-N(CH ₃) ₂	–7.59	–2254.04	Phe-504	–6.84	–1532.68	–
M5	4-Cl	–7.56	–2254.18	Phe-504	–6.81	–1531.56	Asp-248
M6	3,4-(Cl) ₂	–7.57	–2249.96	Phe-504	–6.82	–1532.68	Asp-248
M7	NO ₂	–7.57	–2238.91	–	–6.69	–1522.58	–
M8	3,4-(OCH ₃) ₂	–7.96	–2223.89	Phe-504	–6.99	–1508.00	Asp-248
M9	3,4,5-(OCH ₃) ₃	–7.81	–2238.80	Phe-504	–6.94	–1519.01	Asp-248

TABLE-2
DOCKING SCORE AND DETAILS OF DOCKING RESULTS OBTAINED USING SWISS DOCK

S. No.	R	Trpv1		Interacting residues	Glutamate		Interacting residues
		Energy (ΔG)	Full fitness		Energy (ΔG)	Full fitness	
RN8	–	-8.01	-5032.40	Lys-238	-9.35	-1843.12	Lys-151
ATP				Glu-293			Lys-144
M1	H	-6.48	-1384.24	Tyr-246	-7.24	-1388.30	Asn-242
M2	4-OH	6.95	-1384.93	Glu-210, Arg-211	-7.39	-1390.36	Ser-108
M3	2,3-(OCH ₃) ₂	-6.81	-1385.56	Lys-236	-7.64	-1385.55	Asn-242
M4	4-N(CH ₃) ₂	-6.77	-1371.07				Ser-108
M5	4-Cl	-6.57	-1399.75	Glu-326	-7.62	-1376.11	Pro-105
M6	3,4-(Cl) ₂	-6.81	-1361.33	Tyr-246	-7.55	-1399.96	Asn-242
M7	NO ₂	-6.64	-1386.10	Lys-238	-7.65	-1359.84	Ile-92
M8	3,4-(OCH ₃) ₂	-7.12	-1371.72	–	-7.60	-1388.50	Ser-108
M9	3,4,5-(OCH ₃) ₃	-7.15	-1361.75	Lys-238	-7.99	-1371.24	Asn-242
				Lys-238	-8.01	-1361.68	Asn-242
							Gly-219, Ile-92

electron withdrawing or donating groups is favourable for binding with the receptors. It can also be observed that introduction of 3,4-dimethoxy group is favourable to bind with COX-2 enzyme and glutamate receptors; presence of hydroxy group or 3,4,5-trimethoxy substitution is favourable for binding with P2X3 receptor. With respect to TRPV1 receptors, hydroxy or 3,4-dimethoxy functionalities favour receptor-ligand interactions. Halogen containing derivatives showed moderate interactions with all the targets.

Literature revealed that 3-methyl-4-substituted benzylidene pyrazol-5-ones (**M1-M4**) showed good antiinflammatory and antinociceptive activity in the carrageenan induced inflammatory model and tail flick, acetic acid induced writhing test, respectively [14]. In view of good binding affinity of 3-methyl-4-substituted benzylidene pyrazol-5-ones (**M1-M9**) with TRPV1, P2X3 and glutamate receptors, synthesis was carried out and the compounds were screened for their antinociceptive activity in capsaicin, glutamate and ATP-induced nociception models.

Prediction of molecular and ADME descriptors: Molecular descriptors are associated with oral bioavailability, if molecules obey the "Lipinski rule", it can be predicted that their oral bioavailability will be good (log p \leq 5, molecular weight \leq 500, hydrogen bond acceptors \leq 10 and hydrogen bond donors \leq 5). Predicted values (Table-3) indicated that all the derivatives (**M1-M9**) have obeyed the Lipinski rules of five, suggested that they might have good oral bioavailability (Table-4).

Chemical induced nociception models: The antinociceptive activity of 3-methyl-4-substituted benzylidene pyrazol-5-ones (**M1-M9**) was assessed using chemical induced nociception models such as capsaicin, glutamate and ATP-induced nociception models at a dose of 150 mg/kg body weight by administering orally. Aspirin was used as standard drug at a dose of 100 mg/kg body weight which was administered orally.

Capsaicin induced nociception: In this model, 3,4-dichloro benzylidene derivative (**M6**) displayed highest activity by significantly inhibiting nociceptive behaviour produced by intraplantar injection of capsaicin when compared to the control. Unsubstituted (**M1**) and 4-dimethylamino benzylidene derivative (**M4**) exhibited moderate activity (Fig. 5). Compounds **M6**, **M1** and **M4** showed good binding affinity for TRPV1 receptors (-6.81, -7.04 and -6.85 kcal/mol). The activity of title compounds in this model indicates their possible involvement with vanilloid receptor antagonism. Results indicate that 3-methyl-4-substituted benzylidene pyrazol-5-one possessing chlorine at 3rd and 4th positions was able to produce significant antinociception probably by interacting with TRPV1 receptor. 4-Hydroxy benzylidene derivative (**M2**) showed good binding affinity for TRPV1 receptor (-6.95 kcal/mol) but it was unable to show any significant activity in this model. Mariappan *et al.* [14,15] reported good antinociceptive activity of dimethylamino derivative in tail flick method and carrageenan-induced paw edema tests. The results of present study indicate that this derivative can

TABLE-3
MOLINSPIRATION PROPERTIES OF 3-METHYL-4-SUBSTITUTED BENZYLIDENE PYRAZOL-5-ONES

Compd.	R	Millog P	TPSA	m.w.	nON	nOHNH	n viol	n rot	m.vol	ABS (%)
M1	H	1.51	45.75	186.21	3	1	0	1	171.83	93.21
M2	4-OH	1.03	65.98	202.21	4	2	0	1	179.84	86.23
M3	2,3-(OCH ₃) ₂	1.33	64.22	246.27	5	1	0	3	222.92	86.84
M4	4-N(CH ₃) ₂	1.61	48.99	229.28	4	1	0	2	217.73	92.09
M5	4-Cl	2.19	45.75	220.66	3	1	0	1	185.36	93.21
M6	3,4-(Cl) ₂	2.80	45.75	255.10	3	1	0	1	198.90	93.21
M7	NO ₂	1.47	91.58	231.21	6	1	0	2	195.16	77.40
M8	3,4-(OCH ₃) ₂	1.16	64.22	246.27	5	1	0	3	222.92	86.84
M9	3,4,5-(OCH ₃) ₃	1.14	73.46	276.29	6	1	0	4	248.46	83.65

Millog P- (Lipophilicity); TPSA- (Topological Surface Area); m.w. - (Molecular Weight); ON - (Sum of Hydrogen Bond Receptors); OHNH - (Sum of Hydrogen Bond Donors); n viol (Number of Violations); n rot- (Number of Rotatable Bonds); m.vol -molecular volume.

TABLE-4
ADME PROPERTIES OF 3-METHYL-4-SUBSTITUTED BENZYLIDENE PYRAZOL-5-ONES

Compd.	R	BBB	CaCo2	HIA	MDCK	PPB	SKIN
M1	H	0.84	20.94	95.49	227.93	70.74	-3.1
M2	4-OH	0.43	21.11	91.48	18.94	73.43	-4.2
M3	2,3-(OCH ₃) ₂	0.61	10.84	95.75	70.15	51.64	-3.9
M4	4-N(CH ₃) ₂	0.88	23.26	95.71	161.35	67.41	-3.5
M5	4-Cl	0.94	20.99	95.73	265.47	97.88	-3.2
M6	3,4-(Cl) ₂	0.89	12.32	96.00	192.48	100.00	-3.3
M7	NO ₂	0.27	8.97	85.41	11.27	78.46	-3.7
M8	3,4-(OCH ₃) ₂	0.61	23.87	95.75	127.43	53.02	-3.9
M9	3,4,5-(OCH ₃) ₃	0.47	26.42	95.42	144.54	47.30	-4.0

BBB-(Blood Brain Barrier Penetration); CaCo2- (CaCo2 Cell Permeability); HIA-(Human Intestinal Absorption); MDCK-(Maden Darby Canine Kidney cell permeability); PPB- (Plasma Protein Binding); SKIN- (Skin Permeability)

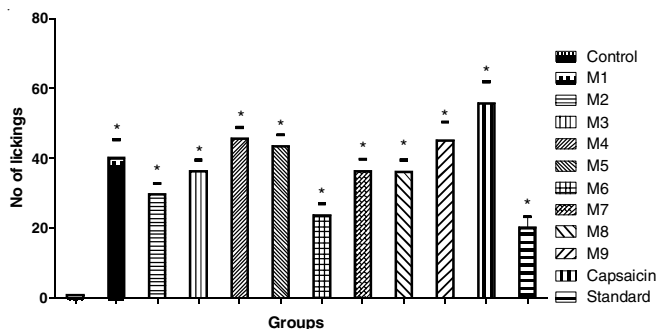


Fig. 5. Antinociceptive effects of title compounds in capsaicin induced nociception model [All values were expressed as Mean \pm SD consisting of six animals; * p < 0.05 compared to control group]

interact with TRPV1 receptors and produce antinociceptive effect.

ATP induced nociception: ATP and its agonists α,β -methylene ATP and 2-methylthio ATP stimulate sensory neurons and known to participate in nociceptive processing [23]. Pain is elicited when ATP is injected *via* intraplantar route in experimental animals, which can be observed in the form of lifting and licking of the injected paw. ATP undergoes degradation by ATP-endonucleotidase enzyme in the *in vivo* experimental conditions and hence nociception can be clearly observed within 10 min after intraplantar injection of ATP [36].

In control animals ATP induced nocifensive behavior was clearly observed for 10 min after intraplantar injection of ATP. Results showed that except few compounds (M2, M3, M5 and M6) were unable to exert any significant activity in this test (Fig. 6). 3,4-Dichloro benzylidene derivative (M6), significantly reduced flinching behaviour induced by ATP suggesting its ability and potency to inhibit the action of ATP. The results suggest that M3, M2 and M8 were able to inhibit the action of ATP. Previous studies [14] have shown that the derivatives possessing chlorine atom or nitro group at 4th position of benzylidene ring displayed good antinociceptive activity in tail flick method, suggested that they are active at the central levels. In present study, these compounds exhibited promising antinociceptive activity in ATP induced model.

Glutamate induced paw licking test: The results (Fig. 7) showed that 3,4,5-trimethoxy benzylidene derivative (M9) significantly reduced licking behaviour at p < 0.05, compared to the control group. Aspirin also caused significant inhibition (p < 0.05). 4-Hydroxy, 2,3-dimethoxy and 3,4-dimethoxy benzylidene derivatives (M2, M3 and M8) displayed good activity

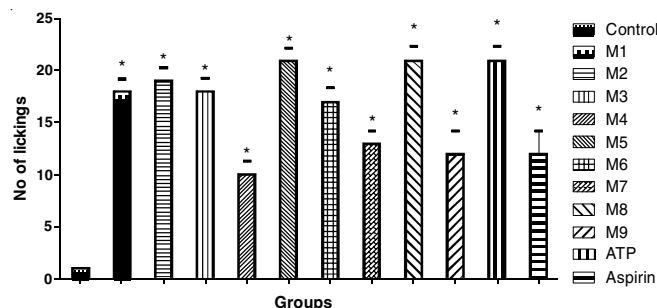


Fig. 6. Antinociceptive effects of title compounds in ATP-induced nociception model [All values were expressed as Mean \pm SD consisting of six animals; * p < 0.05 compared to control group]

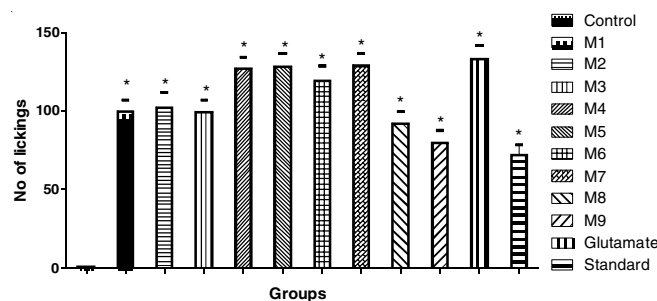


Fig. 7. Antinociceptive effects of title compounds in glutamate-induced nociception model [All values were expressed as Mean \pm SD consisting of six animals; * p < 0.05 compared to control group]

when compared to unsubstituted derivative (M1). Intraplantar injection of glutamate induces peripheral, spinal and supra spinal level nociception by acting on N-methyl-D-aspartate (NMDA) kainate and metabotropic receptors and by NO release [24]. The antinociceptive activity induced by the synthesized compounds in this test might be due to their ability to inhibit any one or more factors. The present study strongly suggests that the antinociceptive activity induced by pyrazolones in glutamate test might be due to their interaction with glutaminergic system or ability to inhibit NO production. The most active derivative (M9) showed highest binding affinity (-7.15 kcal/mol) for glutamate receptor, which is comparable to the reference ligand, RN8 (-8.01 kcal/mol). Compounds M2, M3 and M8 have binding affinities -6.95, 6.76 and -7.02 kcal/mol, respectively suggested that there is a correlation between molecular docking studies and obtained *in vivo* results in this test.

In summary, the present results showed that derivative bearing chlorine atom at both 3rd and 4th positions (M3), elicited antinociception when assessed against both capsaicin and

ATP induced neurogenic pain, whereas 3,4,5-trimethoxy benzylidene derivative displayed highest activity in the glutamate induced paw licking test. 3,4-Dichloro benzylidene derivative was found to be moderately active in glutamate induced nociception.

The results also suggest that presence of chlorine atom is favourable for peripheral antinociceptive activity (capsaicin and ATP induced nociception models), whereas introduction of methoxy group at 3rd and 4th positions or 3rd, 4th and 5th positions was found to favour antinociceptive activity at the central level.

Conclusion

Considering the marked antinociceptive and anti-inflammatory activities of 3-methyl-4-substituted benzylidene pyrazol-5-ones, nine derivatives (**M1-M9**) were synthesized and their antinociceptive activities were evaluated by employing capsaicin, ATP and glutamate induced nociception models. Molecular docking studies on 3-methyl-4-substituted benzylidene pyrazol-5-ones demonstrated that these compounds have good binding affinity for the targets pertaining to antinociception (COX-2, TRPV1, P2X3 and glutamate). Pyrazolone moiety, benzylidene ring and substituent groups (electron withdrawing/releasing) are important determinants for binding with the receptors. Compounds **M6** (3,4-dichloro) and **M8** (3,4-dimethoxy) displayed good antinociceptive activity in TRPV1 and ATP induced nociception models whereas, compound **M9** (3,4,5-trimethoxy) exhibited promising activity in glutamate-induced nociception. The results might be useful to design and develop pyrazolones as potential antinociceptive agents.

ACKNOWLEDGEMENTS

The authors are thankful to DST-CURIE for conducting FTIR analysis.

CONFLICT OF INTEREST

The authors declare that there is no conflict of interests regarding the publication of this article.

REFERENCES

- J.X. Li and Y. Zhang, *Eur. J. Pharmacol.*, **681**, 1 (2012); <https://doi.org/10.1016/j.ejphar.2012.01.017>.
- G.R. Tibbs, D.J. Posson and P.A. Goldstein, *Trends Pharmacol. Sci.*, **37**, 522 (2016); <https://doi.org/10.1016/j.tips.2016.05.002>.
- A.P. Ford, *Purinergic Signal.*, **8**, S3 (2012); <https://doi.org/10.1007/s11302-011-9271-6>.
- A.S. Yekkiral, D.P. Roberson, B.P. Bean and C.J. Woolf, *Nat. Rev. Drug Discov.*, **16**, 810 (2017); <https://doi.org/10.1038/nrd.2017.87>.
- G. Labar, J. Wouters and D.M. Lambert, *Curr. Med. Chem.*, **17**, 2588 (2010); <https://doi.org/10.2174/092986710791859414>.
- S.M. Saario and J.T. Laitinen, *Basic Clin. Pharmacol. Toxicol.*, **101**, 287 (2007); <https://doi.org/10.1111/j.1742-7843.2007.00130.x>.
- S. Hua and P.J. Cabot, *Front. Pharmacol.*, **5**, 211 (2014); <https://doi.org/10.3389/fphar.2014.00211>.
- T.L. Yaksh, S.A. Woller, R. Ramachandran and L.S. Sorkin, *F1000Prime Rep.*, **7**, 1 (2015); <https://doi.org/10.12703/P7-56>.
- J. Barclay, S. Patel, G. Dorn, G. Wotherspoon, S. Moffatt, L. Eunson, S. Abdel'al, F. Natt, J. Hall, J. Winter, S. Bevan, W. Wishart, A. Fox and P. Ganju, *J. Neurosci.*, **22**, 8139 (2002); <https://doi.org/10.1523/JNEUROSCI.22-18-08139.2002>.
- I. Kissin, *Anesth. Analg.*, **110**, 780 (2010); <https://doi.org/10.1213/ANE.0b013e3181cde882>.
- K. Lalit, T. Chandresh and S. Vivek, *Int. J. Res. Pharm. Sci.*, **2**, 13 (2012).
- R. Ramajayam, K.P. Tan, H.G. Liu and P.H. Liang, *Bioorg. Med. Chem.*, **18**, 7849 (2010); <https://doi.org/10.1016/j.bmc.2010.09.050>.
- R. Prajuli, J. Banerjee and H. Khanal, *Orient. J. Chem.*, **31**, 2099 (2015); <https://doi.org/10.13005/ojc/310430>.
- G. Mariyappan, B.P. Saha, L. Sutharson and A. Haldar, *Indian J. Chem.*, **49B**, 1671 (2010).
- G. Mariappan, B.P. Saha, L. Sutharson, A. Singh, S. Garg, L. Pandey and D. Kumar, *Saudi Pharm. J.*, **19**, 115 (2011); <https://doi.org/10.1016/j.jsps.2011.01.003>.
- R. Nassini, C. Fusi, S. Materazzi, E. Coppi, T. Tuccinardi, I.M. Marone, F. De Logu, D. Preti, R. Tonello, A. Chiarugi, R. Patacchini, P. Geppetti and S. Benemei, *Br. J. Pharmacol.*, **172**, 3397 (2015); <https://doi.org/10.1111/bph.13129>.
- S.E. Gulmez, H. Gurdal and F.C. Tulunay, *Pharmacology*, **78**, 202 (2006); <https://doi.org/10.1159/000096688>.
- P. Vicini, F. Zani, P. Cozzini and I. Doytchinova, *Eur. J. Med. Chem.*, **37**, 553 (2002); [https://doi.org/10.1016/S0223-5234\(02\)01378-8](https://doi.org/10.1016/S0223-5234(02)01378-8).
- R. Ottanà, R. Maccari, M.L. Barreca, G. Bruno, A. Rotondo, A. Rossi, G. Chiricosta, R. Di Paola, L. Sautebin, S. Cuzzocrea and M.G. Vigorita, *Bioorg. Med. Chem.*, **13**, 4243 (2005); <https://doi.org/10.1016/j.bmc.2005.04.058>.
- A.A. Chavan and N.R. Pai, *ARKIVOC*, 148 (2007); <https://doi.org/10.3998/ark.5550190.0008.g16>.
- A. Grosdidier, V. Zoete and O. Michielin, *J. Comput. Chem.*, **32**, 2149 (2011); <https://doi.org/10.1002/jcc.21797>.
- H. Knotkova, M. Pappagallo and A. Szallasi, *Clin. J. Pain*, **24**, 142 (2008); <https://doi.org/10.1097/AJP.0b013e318158ed9e>.
- S.G. Hamilton, A. Wade and S.B. McMahon, *Br. J. Pharmacol.*, **126**, 326 (1999); <https://doi.org/10.1038/sj.bjp.0702258>.
- J. Du, M. Koltzenburg and S.M. Carlton, *Pain*, **89**, 187 (2001); [https://doi.org/10.1016/S0304-3959\(00\)00362-6](https://doi.org/10.1016/S0304-3959(00)00362-6).
- A.G. Nerkar, S.A. Kudale, P.P. Joshi and H.U. Chikhale, *Int. J. Pharm. Pharm. Sci.*, **4**, 449 (2012).
- M.Y. Zhao, M.H. Abraham, J. Le, A. Hersey, C.N. Luscombe, G. Beck, B. Sherborne and I. Cooper, *Pharm. Res.*, **19**, 1446 (2002); <https://doi.org/10.1023/A:1020444330011>.
- P.N. Dube, S.S. Bule, S.N. Mokale, M.R. Kumbhare, P.R. Dighe and Y.V. Ushir, *Chem. Biol. Drug Des.*, **84**, 409 (2014); <https://doi.org/10.1111/cbdd.12324>.
- R. Giniatullin and A. Nistri, *Front. Cell. Neurosci.*, **7**, 1 (2013); <https://doi.org/10.3389/fncel.2013.00245>.
- L.A. Alves, J.H.M. da Silva, D.N.M. Ferreira, A.A. Fidalgo-Neto, P.C.N. Teixeira, C. de Souza, E. Caffarena and M. de Freitas, *Int. J. Mol. Sci.*, **15**, 4531 (2014); <https://doi.org/10.3390/ijms15034531>.
- Z. Wang, L. Sun, H. Yu, Y. Zhang, W. Gong, H. Jin, L. Zhang and H. Liang, *Int. J. Mol. Sci.*, **13**, 8958 (2012); <https://doi.org/10.3390/ijms13078958>.
- A. Szallasi, D.N. Cortright, C.A. Blum and S.R. Eid, *Nat. Rev. Drug Discov.*, **6**, 357 (2007); <https://doi.org/10.1038/nrd2280>.
- K. Elokely, P. Velisetty, L. Delemotte, E. Palovcak, M.L. Klein, T. Rohacs and V. Carnevale, *Proc. Natl. Acad. Sci.*, **113**, E137 (2016); <https://doi.org/10.1073/pnas.1517288113>.
- K.M. Wozniak, C. Rojas, Y. Wu and S.B. Slusher, *Curr. Med. Chem.*, **19**, 1323 (2012); <https://doi.org/10.2174/092986712799462630>.
- D. Bleakman, A. Alt and E.S. Nisenbaum, *Semin. Cell. Dev. Biol.*, **17**, 592 (2006); <https://doi.org/10.1016/j.semcdb.2006.10.008>.
- M. Balestra, H. Bunting, D. Chen, I. Egle, J. Forst, J. Frey, M. Isaac, F. Ma, D. Nugiel, A. Slassi, G. Steelman, G.R. Sun, R. Ukkiramapandian, B. Sundar, R.A. Urbanek and S. Walsh, Pyrazolone Compounds as Metabotropic Glutamate Receptor Agonists for the Treatment of Neurological and Psychiatric Disorders, WO2006071730A1 (2005).
- P.A. Bland-Ward and P.P.A. Humphrey, *Br. J. Pharmacol.*, **122**, 365 (1997); <https://doi.org/10.1038/sj.bjp.0701371>.